SI APPENDIX: PLA2G6 guards placental trophoblasts against ferroptotic injury

Authors: Ofer Beharier, Vladimir A. Tyurin, Julie P. Goff, Jennifer Guerrero-Santoro, Kazuhiro Kajiwara, Tianjiao Chu, Yulia Y. Tyurina, Claudette M St Croix, Callen T Wallace, Samuel Parry, W. Tony Parks, Valerian E. Kagan, Yoel Sadovsky

Corresponding author: Yoel Sadovsky, ysadovsky@mwri.magee.edu

This PDF includes the following:

- Supplementary experimental procedures
- Figures and legends S1–S10, (and legend for separate movie file Fig. S6)
- Tables S1–5
- References cited in the supplementary experimental procedures and legends
- Source Data Figures (uncropped histological figures and gels, with inset of formatted figure for reference)

Other supplementary materials for this manuscript include the following:

- Fig. S6 movie file
- Source Data Tables 1 – 3, (separate Excel workbook)

SUPPLEMENTARY EXPERIMENTAL PROCEDURES

Immunofluorescence 4-HNE and TUNEL assay

For PLA2G6 immunofluorescence, placental sections were deparaffinized and rehydrated. Antigen retrieval was performed by boiling 20 min in 10 mM sodium citrate, pH 6.0. Slides were blocked for 1.5 h in PBS + 0.1% Triton X-100, 0.1% Tween 20, 1% BSA, and 5% donkey serum, then incubated overnight with anti-PLA2G6 rabbit polyclonal primary antibody (*SI Appendix,* Table S3). Following PBS/Tween washes, the slides were incubated with donkey anti-rabbit 594 secondary antibody (*SI Appendix*, Table S3) for 1 h, at room temperature (RT). The slides were washed, placed in 10 mM CuSo4 in 50 mM NH4, pH 5 for 40 min at RT. Coverslips were mounted with Fluoromount-G (#00-4958-02, Invitrogen) after DAPI staining, and the slides were imaged using a Nikon 90i widefield microscope. For 4-HNE immunofluorescence, placental samples were fixed in 4% paraformaldehyde, cryoprotected in 30% sucrose and embedded in OCT. Frozen sections were permeabilized with 0.1% Triton-x 100, blocked with 2% BSA in PBS and incubated overnight at 4^0 with 4-HNE monoclonal antibody (Thermo-Fisher #MA5-27570) at 1:50. Following PBS +0.5% BSA wash, the slides were incubated with goat anti-mouse Alexa Fluor 488 2^{ry} antibody at 1:1000 for 60 min at RT. Nuclei were DAPI stained and samples imaged on a Nikon 90i widefield microscope. TUNEL assay was performed using DeadEnd TUNEL system, according to the manufacturer's instructions (Promega).

Western immunoblotting

Cells were washed twice with PBS and lysed in 150 mM NaCl, 20 mM HEPES (Thermo-Fisher), 1% Triton X-100 (USB) and protease inhibitor (Halt Protease Inhibitor Cocktail, Thermo-Fisher), pH 7.4. Proteins were extracted on ice for 15 min, centrifuged at 12,000 g for 25 min at 4°C, and the supernatant was collected. Placental biopsies were snap frozen as detailed above. The tissues were thawed and homogenized using disperser (T10 basic, IKA). Total protein concentration was measured by the Lowry method (Bio-Rad). Extracted proteins (10-40 µg) were separated by SDS-PAGE and transferred to polyvinylidene difluoride membranes (Bio-Rad) as previously described (1). Blots were blocked with 50 mM TBS with 0.1% TBST (Thermo-Fisher) containing 5% nonfat milk for 1 h and incubated overnight at 4°C with antibodies against GPX4, PLA2G6, 15-LOX, ACSL4, PEBP, or actin (*SI Appendix*, Table S3). After washing with TBST, the membranes were incubated with goat anti-mouse HRP-conjugated secondary antibody (*SI Appendix*, Table S3) for 1 h, at RT. A chemiluminescent signal was detected by the ChemiDoc MP Imaging System (BioRad).

RNA extraction and RT-quantitative PCR (RT-qPCR)

Total RNA was extracted from mouse tissues using TRI Reagent (Molecular Research Center) according to the manufacturer's instructions, with added DNase (Thermo), and reverse transcription and quantitative PCR were performed in 384-well plates as we previously described (2, 3). Samples were compared to a control sample by the $2^{-\Delta\Delta Ct}$ method (4). L32 was used as a control transcript. The specificity of amplification was confirmed using a dissociation curve of each PCR product. All primer sequences are provided in *SI Appendix* Table S1.

Imaging and analysis of intracellular oxidized lipid propagation

Analysis of the fraction of fluorescence positive cellular area was performed using the GA3 function NIS Elements. The analysis was using whole high resolution (60X, 1.4NA) large area montage for each time point. To segment out the total cellular area, we used edge detection on the DIC channel followed by intensity thresholding and calculated the total binary area (presented as red). For the Liperfluo data, we measured the background levels at 200 greyscales across all conditions and segmented the data such that that values above that level were defined as above threshold and counted as a positive signal (green in the image) to generate the binary mask. We then calculated the area of positive Liperfluo signal as the total binary area for the Liperfluo channel and expressed this as a fraction of the total cellular area.

Assessment of maternal toxicity after (1S,3R)-RSL3 injection.

After injection of (1S,3R)-RSL3 we assessed the following parameters: (a) maternal survival, determined daily following treatment, (b) maternal weight gain, determined on E0, E13.5, E14.5 and E17.5, (c) stress related behavior, assessed daily by 10 min observation after treatment. Grooming, paw lifting, and disorder of movement or spontaneous standing avoidance were considered as stress or pain related behaviors.

SUPPLEMENTARY FIGURES AND LEGENDS

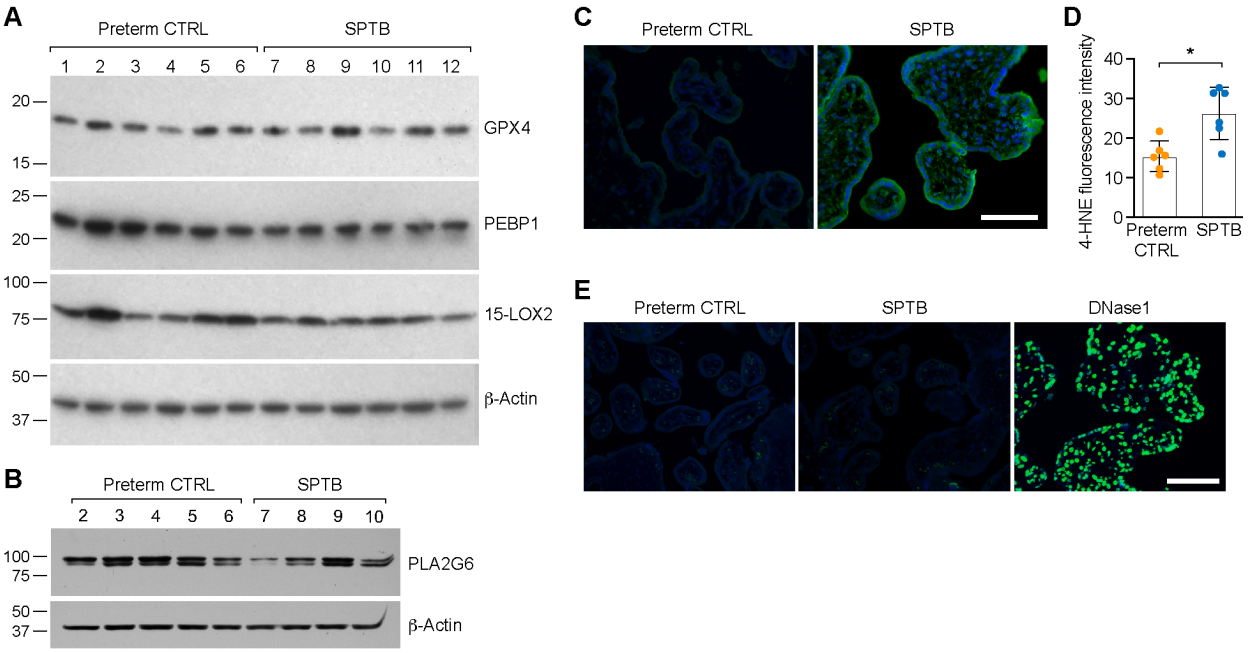

Fig. S1: The expression of key ferroptosis regulators in human placentas complicated by SPTB. (*A*) GPX4, PEBP1, 15-LOX2 and β-actin expression in of SPTB (n=6) and matched preterm control (n=6) placentas. Placenta lysates were used as shown. (*B*) PLA2G6 expression in SPTB (n=5) and matched preterm control (n=4) placentas. Patient numbers correspond between *A* and *B* (see title). The expression of the different proteins was not significant different among the groups (unpaired two-tailed t test). (*C*) Representative images of 4-HNE (green) and DAPI (blue) immunofluorescence in human placental villi of SPTB and preterm control, performed as detailed in Methods. (*D*) Quantitative analyses of 4-HNE immunofluorescence in human placental villi of SPTB and preterm (n=6 for each group). For each sample, data represent the mean ±SD from 4-7 randomly selected fields. **P*<0.01, unpaired t test. (*E*) Representative TUNEL staining (green) of SPTB, preterm control, and preterm control human placental villi exposed to DNase1 (positive control), as detailed in Methods (Bar =100 μm).

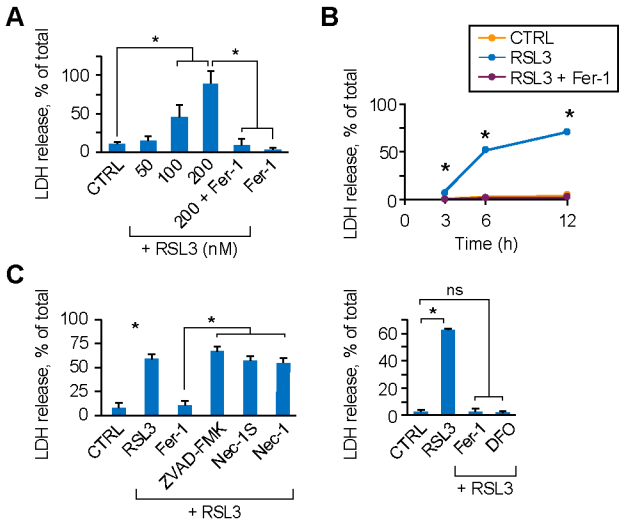

Fig. S2: Inhibition of GPX4 promotes ferroptosis in BeWo cells. (*A*) RSL3-induced concentration-dependent cell death in BeWo cells, measured by relative LDH release. Ferroptosis is blocked by the ferroptosis inhibitor ferrostatin-1 (Fer-1, 0.5 μM). (*B*) RSL3-induced cell death in BeWo cells, measured by relative LDH release. Death is blocked by Fer-1 (0.5 μM). (*C*) The effect of cell death inhibitors on RSL3-induced ferroptosis in BeWo cells. Cells were exposed to RSL3 (200 nM, 24 h) in the absence or presence of Fer-1 (0.5 μM), the pan-caspase inhibitor ZVAD-FMK (20 μM), the necroptosis inhibitors necrostatin-1S (Nec-1S, 50 μM) or necrostatin-1 (Nec-1, 50 μM). Right panel, the effect of the iron chelator deferoxamine (DFO, 100 μM) on RSL3-induced ferroptosis (200 nM, 24 h). The data in this figure represent the mean ±SD of at least 3 independent experiments. Analysis was performed using LME models with Holm's method for multiple comparisons (*A*, *B*, left panel of *C*) and one-way ANOVA with Dunnett's method for multiple comparisons (right panel of *C*). ns, not significant, * $P<0.01$.

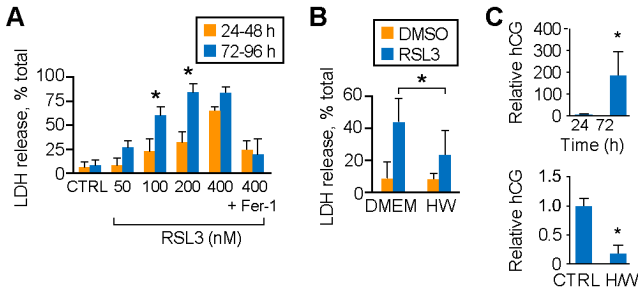

Fig. S3. Trophoblast differentiation enhances RSL3-induced ferroptosis. (*A*) The effect of PHT cell differentiation over time on RSL3-induced cell death. Cell death was measured as LDH release. Death was blocked by ferrostatin-1 (Fer-1, 0.5 μM). **P*<0.05, LME model with Holm's method for multiple comparisons. (*B*) The effect of H/W medium, used to hinder PHT cell differentiation, on the sensitivity to RSL3 (50 nM)-induced ferroptosis. **P*<0.05, two-way ANOVA, with Sidak's post-hoc test. (*C*) The release of hCG to the cell culture medium, serving to validate PHT differentiation conditions. **P*<0.05, t test. Data represent the mean ±SD, n=3.

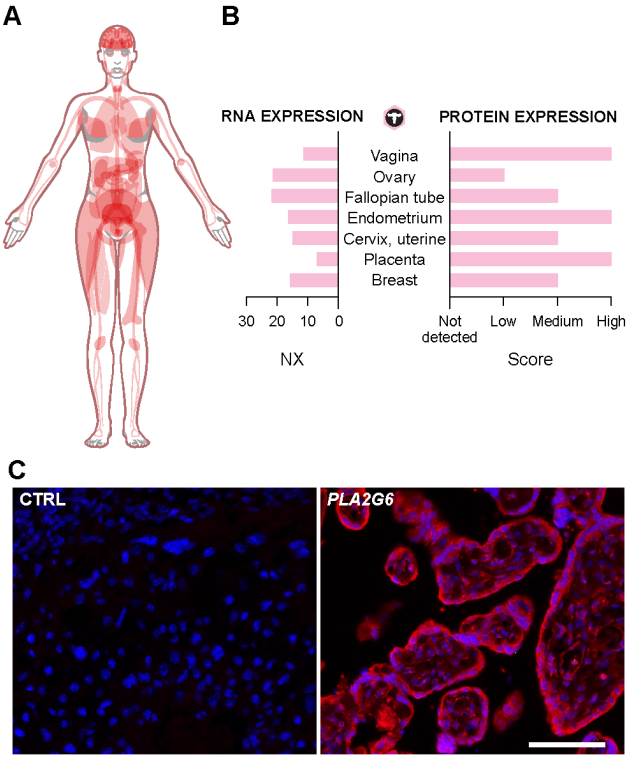

Fig. S4. The expression of PLA2G6 in human female reproductive system and the placenta. (*A*) Expression of PLA2G6 in the human female, represented in red scale. (*B*) The expression of PLA2G6 in human female tissues (left, RNA; and right, protein). Images are from the Human Protein Atlas (Uhlen M, et al. Proteomics. Tissue-based map of the human proteome. *Science.* 2015;347(6220):1260419, www.proteinatlas.org/ENSG00000184381-PLA2G6/tissue, available from v19.3.proteinatlas.org). (*C*) The expression of PLA2G6 protein in the human placental villi, performed by immunofluorescence as detailed in the Methods. Left panel: Control (no primary antibody), Right panel: PLA2G6 (Bar =25 μm).

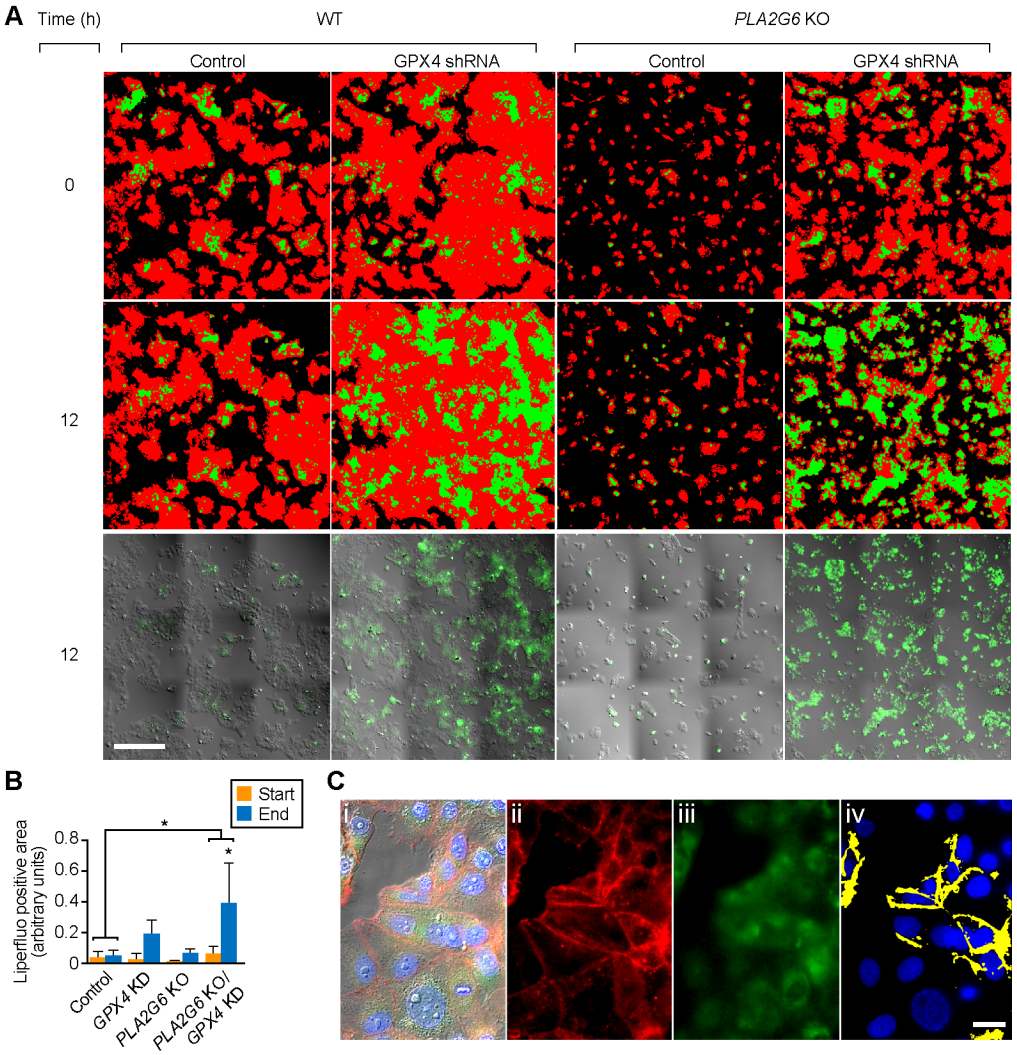

Fig. S5. The propagation of Liperfluo fluorescence following RSL3-induced ferroptosis stimulation by. (*A*) Representative images of total cellular area (red fluorescence) and % Liperfluo positive cellular area (green fluorescence), in the beginning (0 h) and end (12 h) of the experiment (Bar =100 μm). (*B*) Quantitative analysis of the relative Liperfluo fluorescence in panel A, for 0 h and 12 h of experiment. The difference between start and end for each paradigm were determined using linear regression model, with Holm's method for multiple comparisons. The difference among the four paradigms was determined using one-way ANOVA with Tukey's method for multiple comparisons. **P*<0.05 for both analyses. (*C*) Colocalization of Liperfluo fluorescence and cell membrane in KO *PLA2G6* BeWo cells, following 3 h of RSL3 (200 nM). Panel *Ci* shows the differential contrast (DIC) image, *Cii*, CellMask deep red (Invitrogen, in red), *Ciii*, Liperfluo (green), *Civ*, colocalization of CellMask and Liperfluo, with DAPi for nuclei. The images were taken using a 60X (1.4NA optic) magnification. Co-localization was performed using NIS Elements (Nikon Inc., n=3 stage positions). Data for CellMask deep red and Liperfluo were segmented based on emission intensity. The degree of overlap was assessed using a binary "having" statement. The data showed that 85±14% of the cell membrane compartment was positive for Liperfluo, and 31±19% of the Liperfluo signal co-localized with the membrane marker CellMask (Bar: 25 μm).

Fig. S6. A movie showing live cell Liperfluo fluorescence imaging of lipid hydroperoxides in BeWo cells. The experiment was conducted as in Fig. 3*E* and evaluated over 12 h after removal of ferrostatin-1. See uploaded movie file.

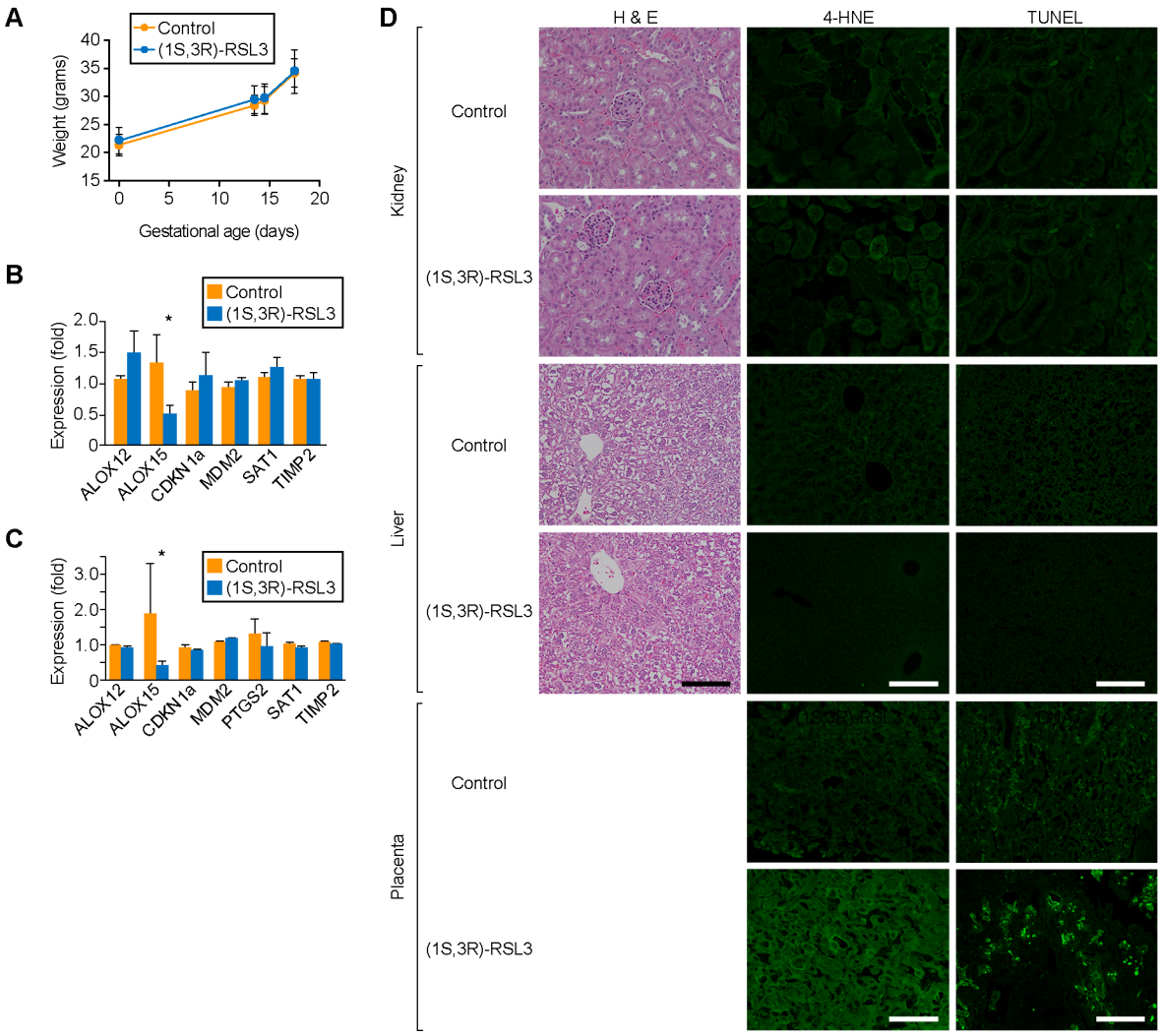

Fig. S7. Assessment of toxic effects of (1S,3R)-RSL3. The effect of intraperitoneal injection of (1S,3R)-RSL3 (25 mg/kg, n=15) *vs* vehicle control (n=10) was assessed on (*A*) maternal weight gain after injection at E13.5 and 14.5. (*B-C*) The expression of transcripts for ferroptotic (*Ptgs2, Alox12, Alox15, and Sat1*), and tissue injury markers (*Mdm2, P21, Timp-2*) in the maternal kidney (*B*) and liver (*C*) (see *SI Appendix* references (5-9). **P*<0.05, two-way ANOVA with Tukey's method for multiple comparisons, n=3. (*D*) Representative images (n=4) of H&E (left), 4-HNE (middle) and TUNEL (right) stains, of the kidney (top) and liver (bottom). Control *Pla2g6*^{KO} placental stains for TUNEL and 4-HNE are also shown. Dams received intraperitoneal injection of vehicle or 25 mg/kg of (1S,3R)-RSL3 at E13.5 and 14.5, and tissues were harvested at E17.5. (Bar =100 μm).

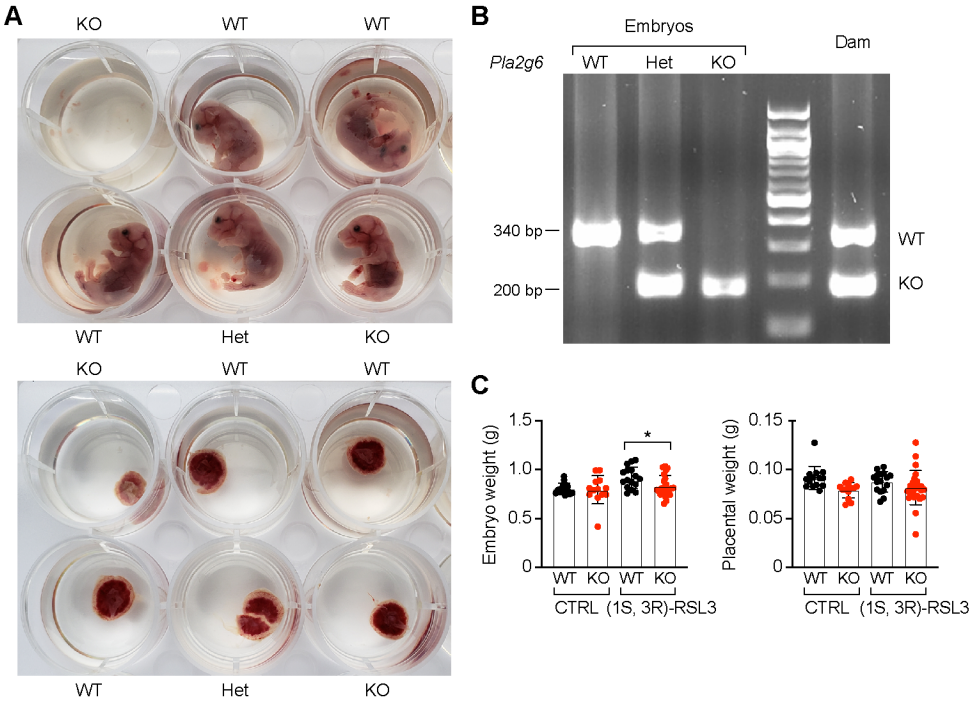

Fig. S8. The effect of GPX4 inhibition by RSL3 on the placenta and embryo. (*A*) Embryos (top) and placentas (bottom) from a representative litter, injected with 25 mg/kg (1S,3R)-RSL3 at E13.5 and E14.5 and harvested at E17.5. One of two *Pla2g6*^{KO} embryos was resorbed, leaving only the residual placenta. The second *Pla2g6*^{KO} pregnancy displayed smaller placentas compared to WT placentas. (*B*) Representative genotype PCR result from *Pla2g6*^{WT}, *Pla2g6*^{Het}, and *Pla2g6*^{KO} embryos and the *Pla2g6*^{Het} dam. (*C*) Embryo (left) and placental (right) weights, collected at E17.5 from *Pla2g6*^{WT} treated with vehicle (n=14) or (1S,3R)-RSL3, (n=18) and *Pla2g6*^{KO} treated with vehicle (n=12) or (1S,3R)-RSL3, (n=25). Data represent mean ±SD. **P*<0.05, two-way ANOVA, with Holm's method for multiple comparisons.

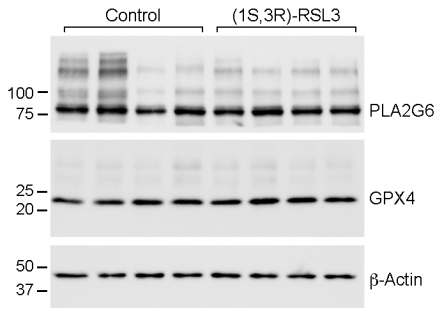

Fig. S9. The effect of (1S,3R)-RSL3 on GPX4 and PLA2G6 protein expression in mouse placentas. GPX4, PLA2G6 and β-Actin expression in WT placenta tissue obtained at E17.5, following IP injection of vehicle (DMSO) control (n=4, placentas from 2 different litters) or (1,3)-RSL3 BeWo (25 mg/kg) at E13.5 and 14.5 (n=4, placentas from 2 different litters).

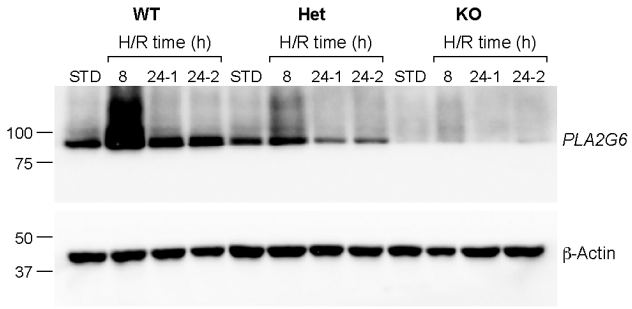

Fig. S10. The expression of PLA2G6 in *Pla2g6 WT, Het* or *KO* placentas. Placental PLA2G6 expression, following hypoxia E11.5-E17.5 and indicated duration of reoxygenation. As expected, *PLA2G6*^{Het} placentas expressed a lower level of PLA2G6 compared to WT.

SI APPENDIX TABLES

Table S1: Clinical characteristics of study participants.

ID#	Gest age (wks)	Gravidity	OB diagnosis	Additional diagnosis	Delivery	5 min APGAR	Birth weight (gm)	Placenta weight (gm)	Sex	Placental histopathology
Spontaneous preterm birth										
1	32	1	Spont preterm labor		Vaginal	7	1600	414	M	Acute chorioamnionitis
2	30	1	Spont preterm labor	Breech	Cesarean	8	1360	420	M	Maternal vascular malperfusion
3	35	1	Spont preterm labor	Breech, Asthma	Cesarean	9	2650	544	F	Maternal vascular malperfusion
4	31	1	Spont preterm labor	Asthma	Vaginal	8	1469	325	F	Maternal vascular malperfusion
5	35	3	Spont preterm labor	Hx of pulmonary emboli	Vaginal	9	2125	446	F	Maternal vascular malperfusion
6	31	1	Spont preterm labor	Obesity	Vaginal	7	1380	354	F	Maternal vascular malperfusion, synt knots, villous hypoplasia
7	29	1	Spont preterm labor		Vaginal	8	1452	440	F	Normal
8	34	3	Spont preterm labor	Bipolar disorder	Vaginal	7	2891	703	M	Normal
9	27	2	Spont preterm labor	PROM	Vaginal	10	998	413	M	Mild maternal vascular malperfusion
10	34	1	Spont preterm labor	Sjorgen Syndrome	Cesarean	9	2008	488	F	Mild maternal vascular malperfusion
11	35	1	Spont preterm labor	Anxiety	Vaginal	9	2805	501	F	Mild maternal vascular malperfusion
Mean	**32**						**1885**	**459**	**63%**	**Female**
Preterm control										
12	35	2	Breech	PROM, no labor	Cesarean	8	2840	572	M	Maternal vascular malperfusion
13	34	1	FHT decelerations	Obesity, anemia	Cesarean	8	2003	496	F	Maternal vascular malperfusion
14	34	5	Worsening HTN	Gestational HTN	Cesarean	7	2784	458	M	Mild maternal vascular malperfusion
15	35	2	Vasa previa		Cesarean	9	2646	584	M	Normal
16	28	3	Abnormal fetal Doppler	FGR, Club foot	Cesarean	8	1000	208	M	Mild maternal vascular malperfusion
17	30	4	Chest pain, NR-FHT	History of preterm birth	Cesarean	8	1056	332	F	Normal
18	35	5	NR-FHTs	History of Cesarean x2	Cesarean	9	2080	692	F	Normal
19	33	3	PROM	Depression, breech	Cesarean	7	1784	486	F	Normal
20	32	4	PROM	Preeclampsia, FGR	Cesarean	8	1112	215	F	Normal
21	34	2	Elective CS	Panic attack, T2DM	Cesarean	8	2330	460	M	Maternal vascular malperfusion
Mean	**33**						**1964**	**450.3**	**50%**	**Female**

Table S2: Sex distribution among 56 surviving fetuses, at E17.5 following IP injection of 25-50 mg/kg of (1S, 3R)-RSL3 at E13.5 and E14.5 (p = ns, Chi Square test).

Sex	*PLA2G6*^{WT}	*PLA2G6*^{Het}	*PLA2G6*^{KO}
Male	5 (55.6%)	16 (52.9%)	7 (53.8%)
Female	4 (44.4%)	18 (47.1%)	6 (46.2%)

Table S3. List of antibodies used in this study.

Protein	Species	Concentration/ Dilution	Vendor	Catalog	RRID
PLA2G6	Rabbit	1:50 (IF)	Sigma Aldrich	HPA001171	AB_1079145
GPX4	Mouse	1 µg/ml (WB)	Santa Cruz	166570	AB_2112427
PLA2G6	Mouse	1 µg/ml (WB)	Santa Cruz	376563	AB_11150308
15-Lox	Mouse	1 µg/ml (WB)	Santa Cruz	271290	AB_10609897
ACSL4	Mouse	1 µg/ml (WB)	Santa Cruz	365230	AB_10843105
PEBP1	Mouse	1 µg/ml (WB)	Santa Cruz	376925	N/A
Actin	Mouse	1:10,000 (WB)	Millipore	MAB1501	AB_2223041
Anti-rabbit (594)	Donkey	1:300 (IF)	Invitrogen	A21207	AB_141637
Anti-Mouse (HRP)	Goat	1:10,000 (WB)	Thermo-Fisher	AB6789	AB_955439
Anti-Mouse (488)	Goat	1:1000 (IF)	Thermo-Fisher	A-11017	AB_2534084
4-HNE	Mouse	1:50 (IF)	Thermo-Fisher	MA5-27570	AB_2735095

Table S4: Sequence of single guide RNA (gRNA) used in the study.

Gene	Name	Sequence (5' – 3')
PNLPA9 (*PLA2G6*)	gRNA-1	CACCGCTCCCGAACTCGGTCACTCG
	gRNA-2	AAACCGAGTGACCGAGTTCGGGAGC
PNPLA2 (*ATGL*)	gRNA-1	CACCGCTTCTCGCGGGGAAACATCG
	gRNA-2	AAACCGATGTTTCCCCGCGAGAAGC
	gRNA-3	CACCGCACGCACATCTACGGCGCCT
	gRNA-4	AAACAGGCGCCGTAGATGTGCGTGC

Table S5: Primer sequences used for genotyping (PCR), sex determination, and tissue injury (qPCR).

Direction/Name	Species	Product length (bp)	Sequence (5' – 3')
PLA2G6 F1	Mouse		CAAATGCACGTTTGGTGTGT
PLA2G6 F2- wild type	Mouse	340	CTCCCTGACCAGGACTGACT
PLA2G6 R- KO	Mouse	200	CTCCAGACTGCCTTGGGAAAA
SRY F	Mouse		GTTCAGCCCTACAGCCACAT
SRY R	Mouse	261	ATCTCTGTGCCTCCTGGAAA
ALOX12-F	Mouse		GATCACTGAAGTGGGGCTGT
ALOX12-R	Mouse		CACACATGGTGAGGAAATGG

Direction/Name	Species	Product length (bp)	Sequence (5' – 3')
ALOX15-F	Mouse		CGGTCTACTTGTCTCCCTGC
ALOX15-R	Mouse		ATCCGCTTCAAACAGAGTGC
Cdkn1a-F (P21)	Mouse		AAGTGTGCCGTTGTCTCTTCG
Cdkn1a-R (P21)	Mouse		AGTCAAAGTTCCACCGTTCTCG
MDM2-F	Mouse		TGTGAAGGAGCACAGGAAAA
MDM2-R	Mouse		TCCTTCAGATCACTCCCACC
mPTGS2-f	Mouse		ATGAGCACAGGATTTGACCA
mPTGS2-R	Mouse		TGGGCTTCAGCAGTAATTTG
SAT1-F	Mouse		GGCTAAATTTAAGATCCGTCCA
SAT1-R	Mouse		CATGTATTCATATTTAGCCAGTTCCTT
Timp2 -F	Mouse		GGCTGTGAGTGCAAGATCACTCG
Timp2 -R	Mouse		GCCTGGTGCCCATTGATGCTCT
L32-F	Mouse		CCTCTGGTGAAGCCCAAGATC
L32-R	Mouse		TCTGGGTTTCCGCCAGTTT

REFERENCES CITED IN *SI APPENDIX*

1. W. T. Schaiff, et al., Peroxisome proliferator-activated receptor-gamma modulates differentiation of human trophoblast in a ligand-specific manner. *J. Clin. Endocrinol. Metab.* **85**, 3874-3881 (2000).
2. T. Mishima, E. Sadovsky, M. E. Gegick, Y. Sadovsky, Determinants of effective lentivirus-driven microRNA expression in vivo. *Sci. Rep.* **6**, 33345 (2016).
3. L. Xie, et al., C19MC microRNAs regulate the migration of human trophoblasts. *Endocrinology* **155**, 4975-4985 (2014).
4. K. J. Livak, T. D. Schmittgen, Analysis of relative gene expression data using real-time quantitative PCR and the 2(-Delta Delta C(T)) Method. *Methods* **25**, 402-408 (2001).
5. W. S. Yang, et al., Regulation of ferroptotic cancer cell death by GPX4. *Cell* **156**, 317-331 (2014).
6. W. S. Yang, et al., Peroxidation of polyunsaturated fatty acids by lipoxygenases drives ferroptosis. *Proc. Natl. Acad. Sci. U. S. A.* **113**, E4966-4975 (2016).
7. Y. Ou, S. J. Wang, D. Li, B. Chu, W. Gu, Activation of SAT1 engages polyamine metabolism with p53-mediated ferroptotic responses. *Proc. Natl. Acad. Sci. U. S. A.* **113**, E6806-E6812 (2016).
8. I. Lopez, A. S. Tournillon, K. Nylander, R. Fahraeus, p53-mediated control of gene expression via mRNA translation during Endoplasmic Reticulum stress. *Cell Cycle* **14**, 3373-3378 (2015).
9. I. Ingold, et al., Selenium utilization by GPX4 is required to prevent hydroperoxide-induced ferroptosis. *Cell* **172**, 409-422 e421 (2018).

Fig. 1*E*

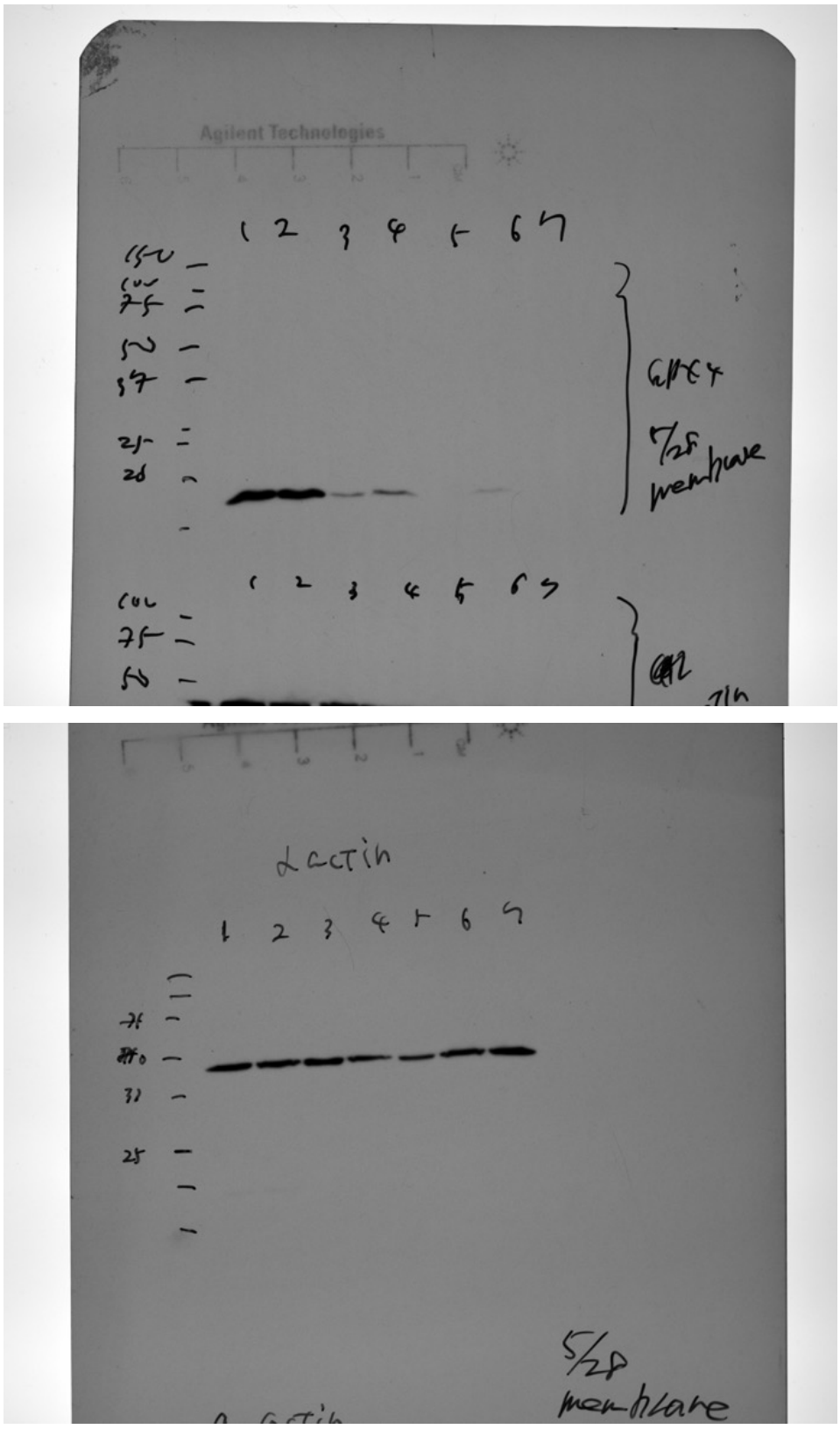

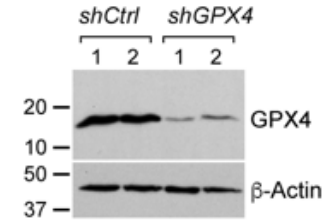

Files:
ofer 2019-10-11 14h37m41s(Silver Stain)
ofer 2019-10-11 14h38m45s(Silver Stain)

Fig. 3*A*

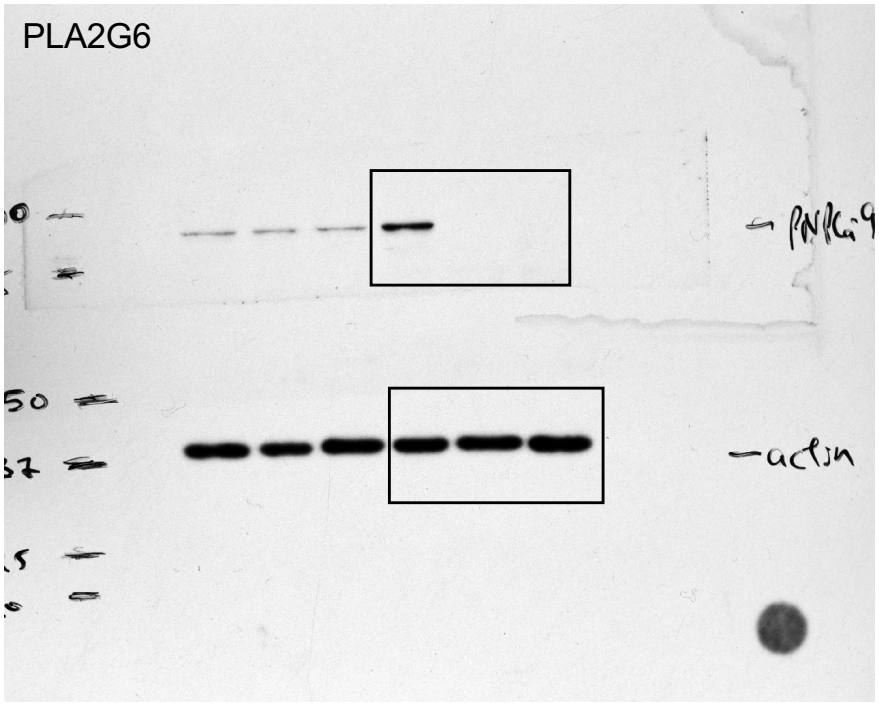

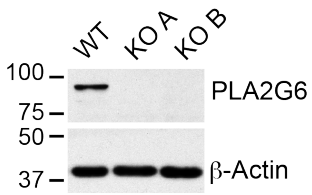

Files:
Fig3a – PLA2G6 wt and ko

Fig. 3*H*

PLA2G6

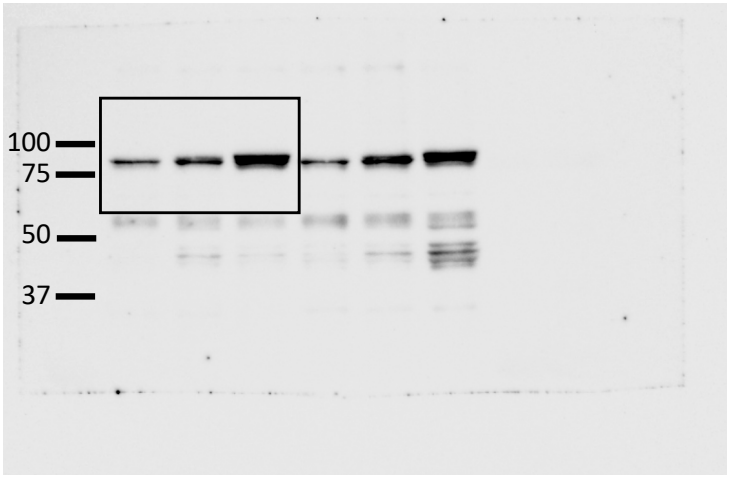

GPX4

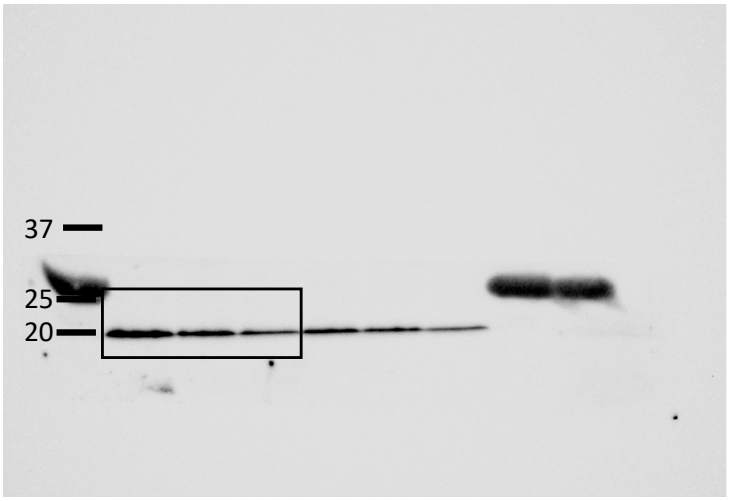

β-Actin

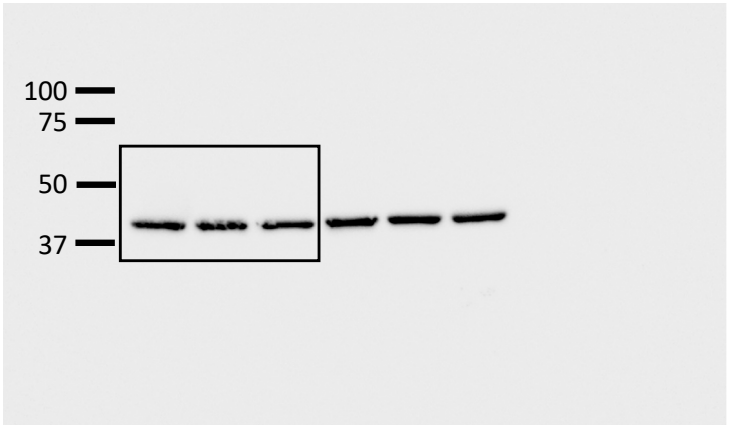

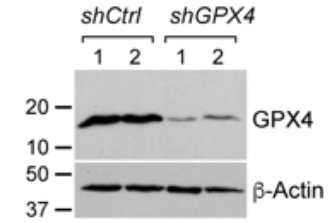

Files:
FIG S3DPLA2G6
PHTB GPX4(Chemiluminescence)
FIG S3D ACTIN

Fig. 4*F*

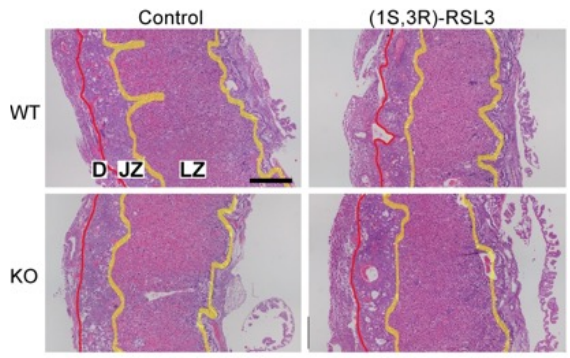

R-370-8 WT Control

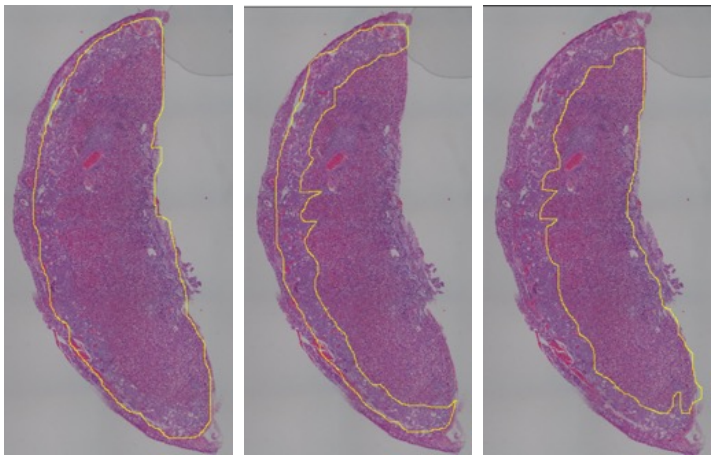

Total JZ LZ

R372-5 WT RSL3

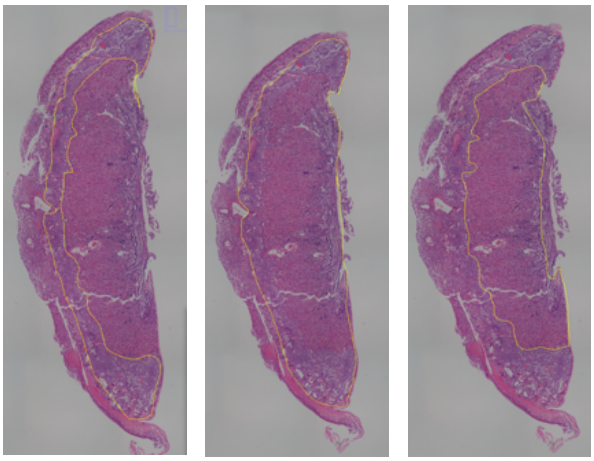

Total JZ LZ

R371-1 KO Control

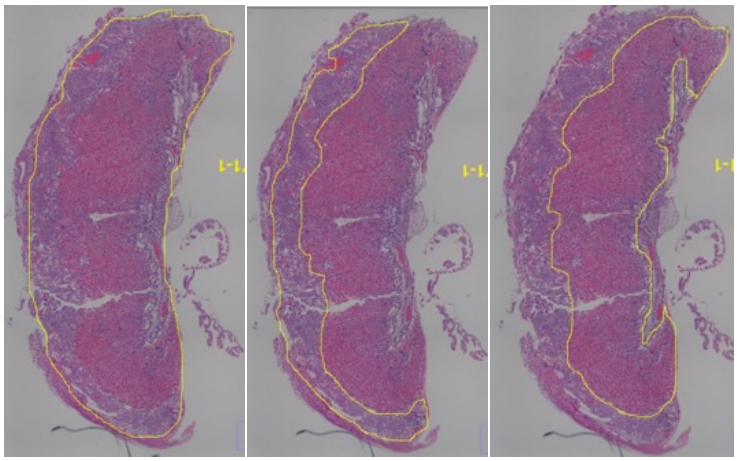

Total JZ LZ

R350-3-5 KO RSL3

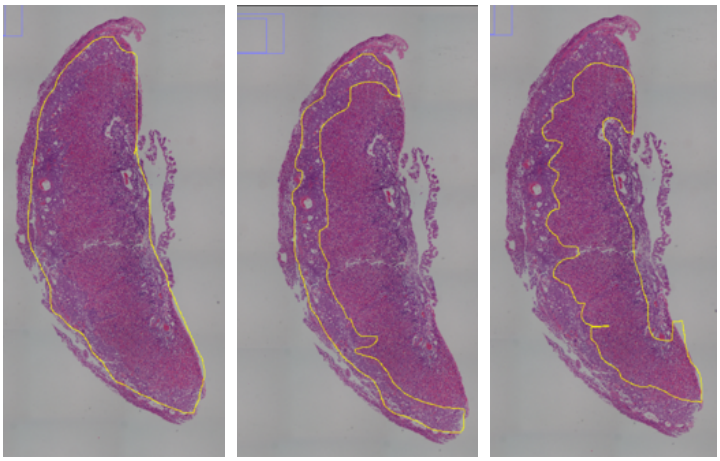

Total JZ LZ

SI Appendix, Fig. S1*A*

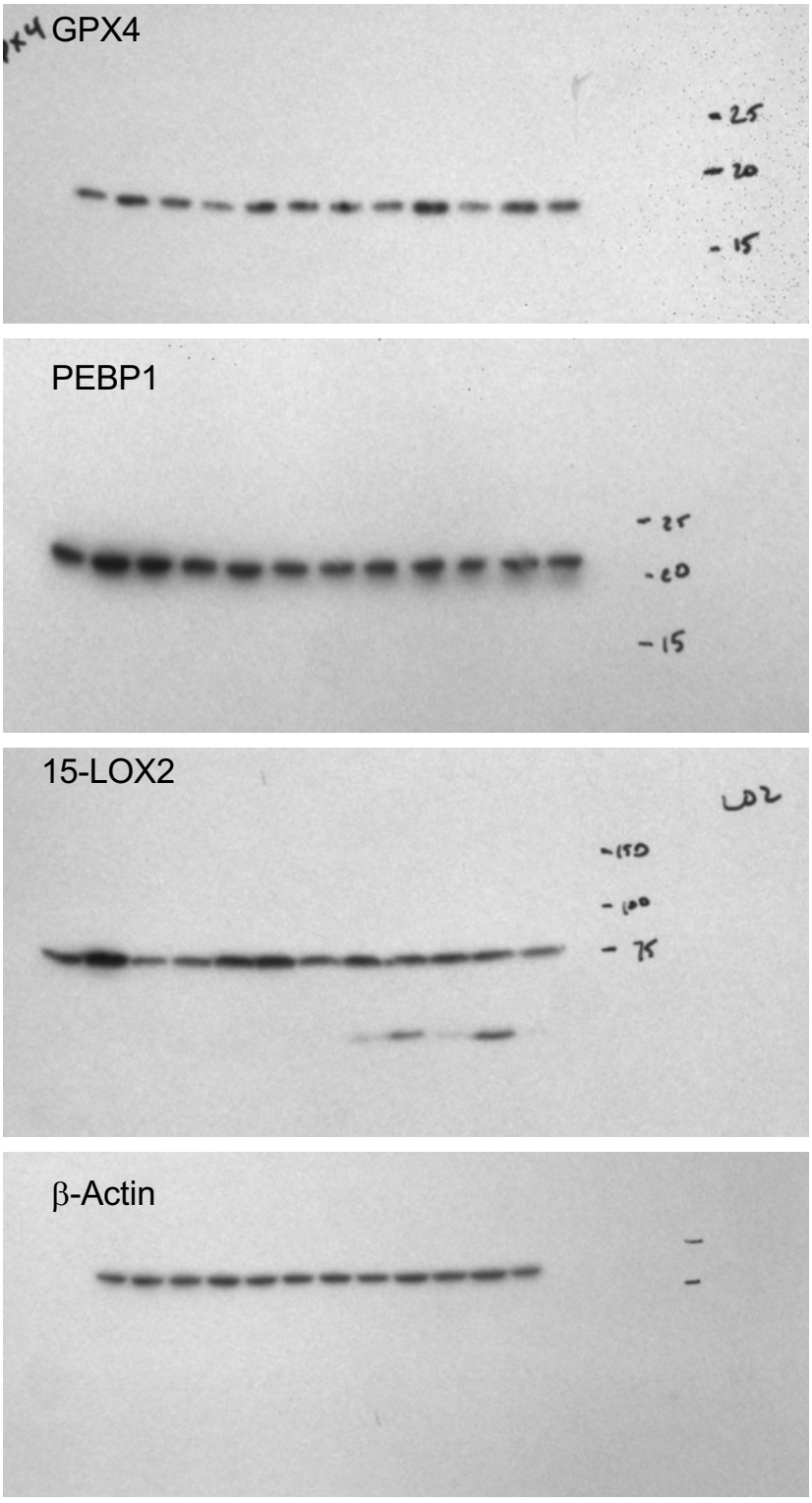

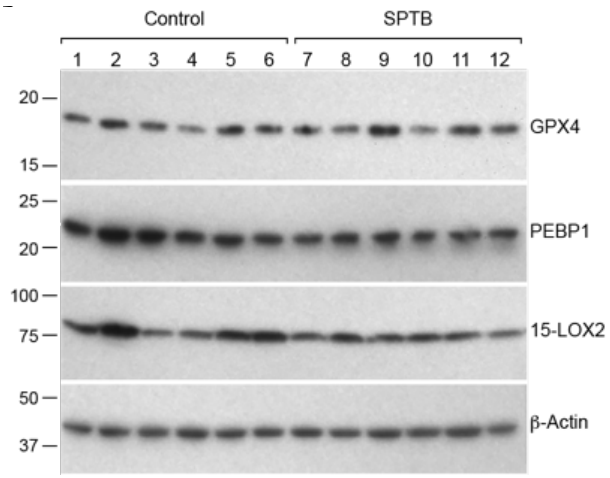

Files:
11 22 17 PEBP1
11 22 17 gpx4
11 22 LO2
11 22 17 actin

SI Appendix, Fig. S1*B*

PLA2G6

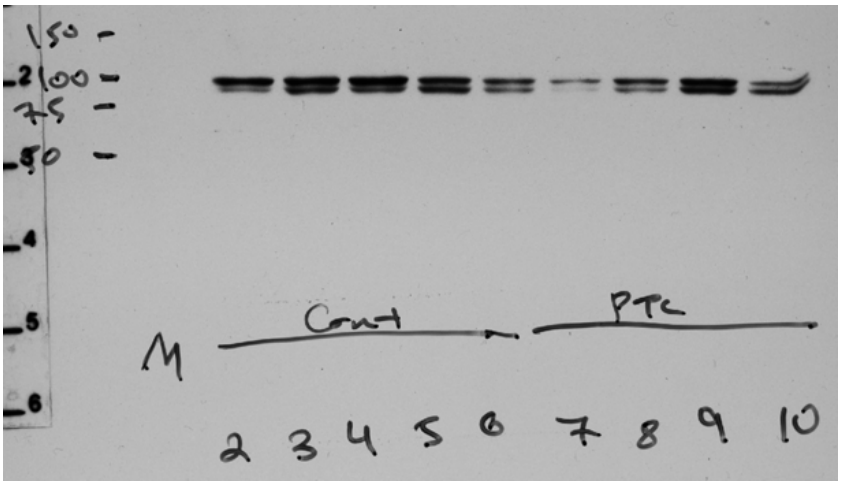

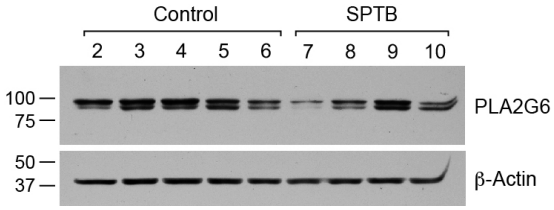

Files:
ofer 2020-20-21 15h14m15s(Coomassie Blue)
ofer 2020-02-21 15h15m30s(Coomassie Blue)

β-Actin

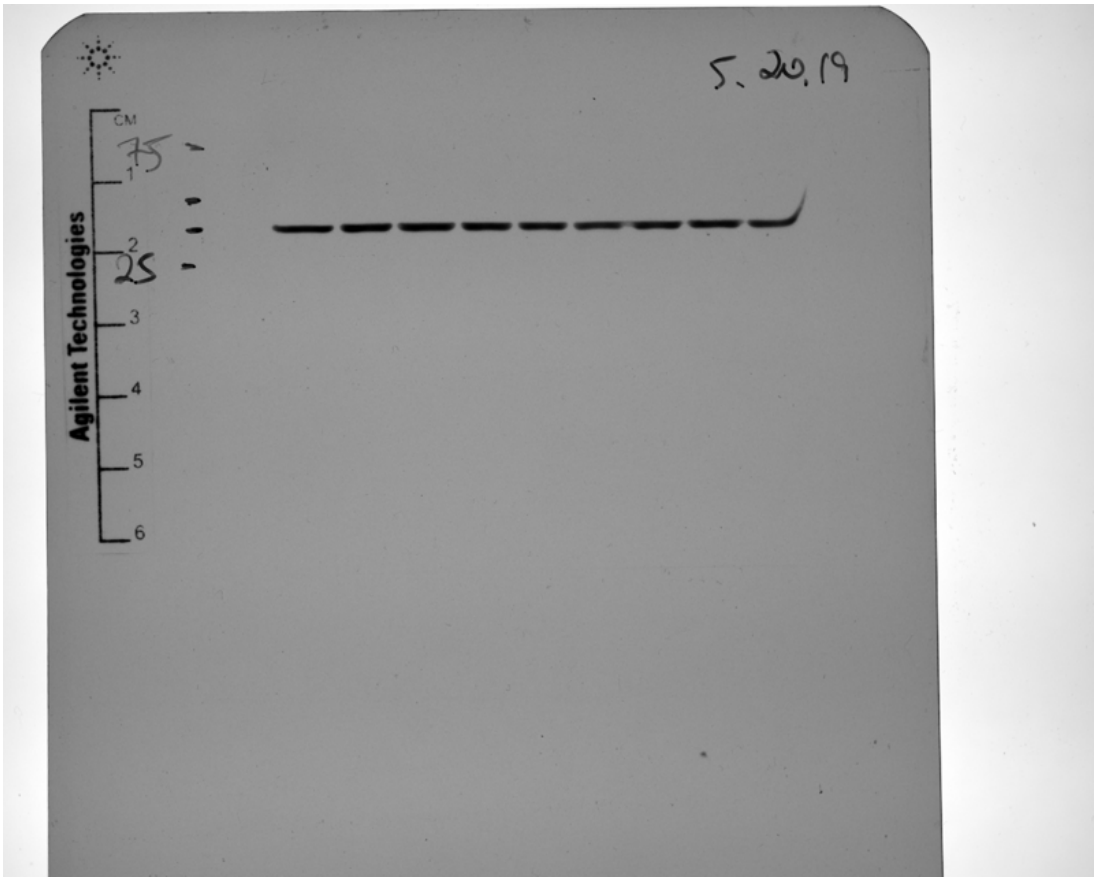

SI Appendix, Fig. S8*B*

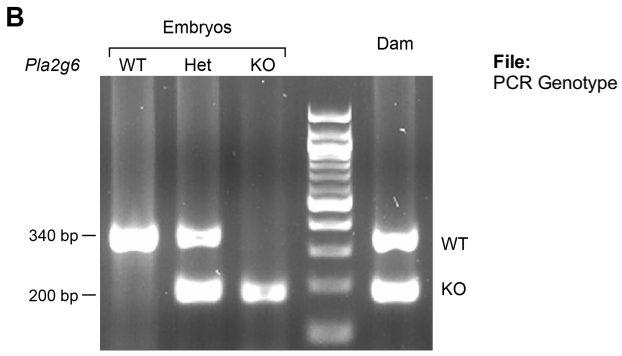

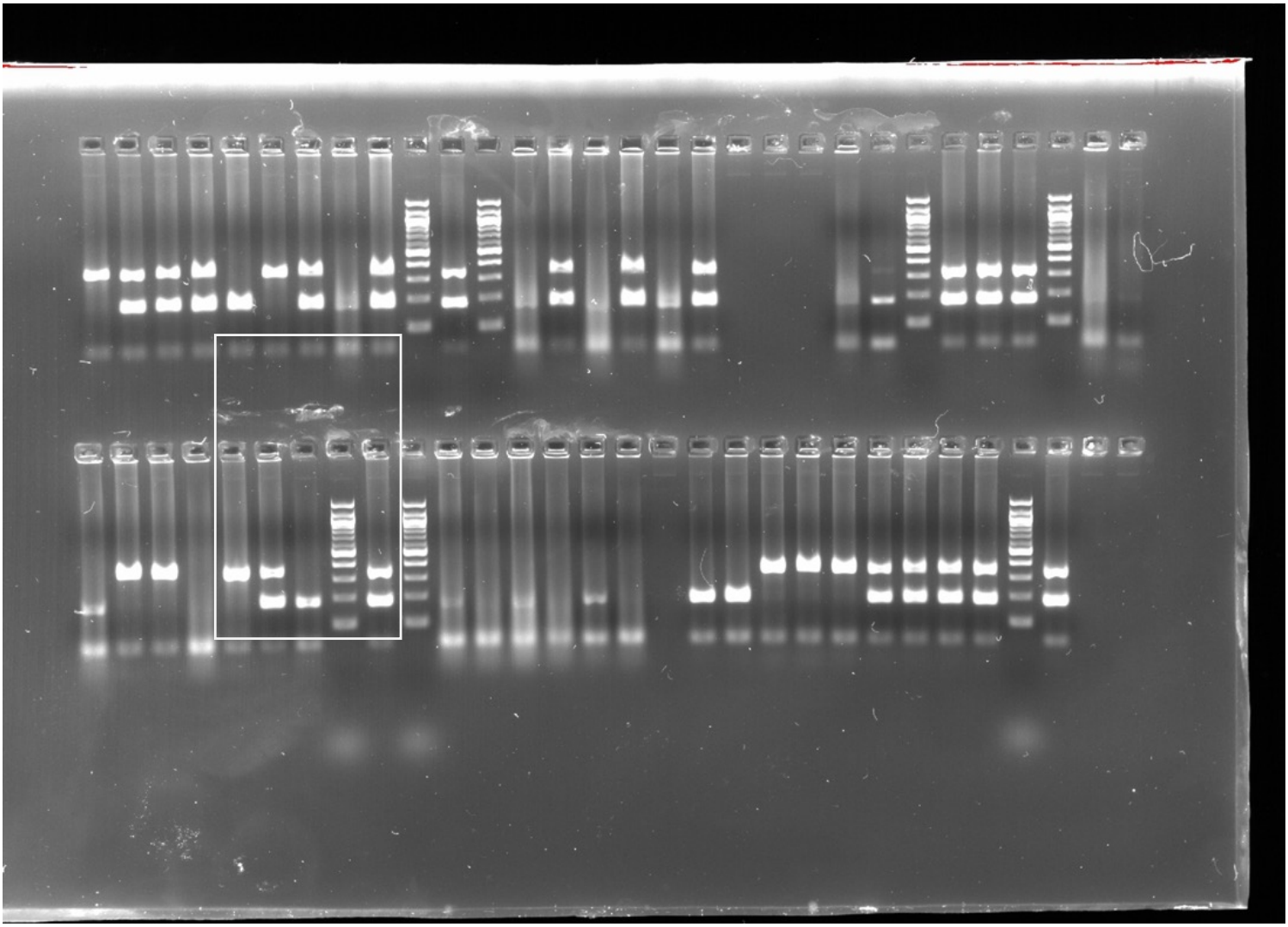

SI Appendix, Fig. S9

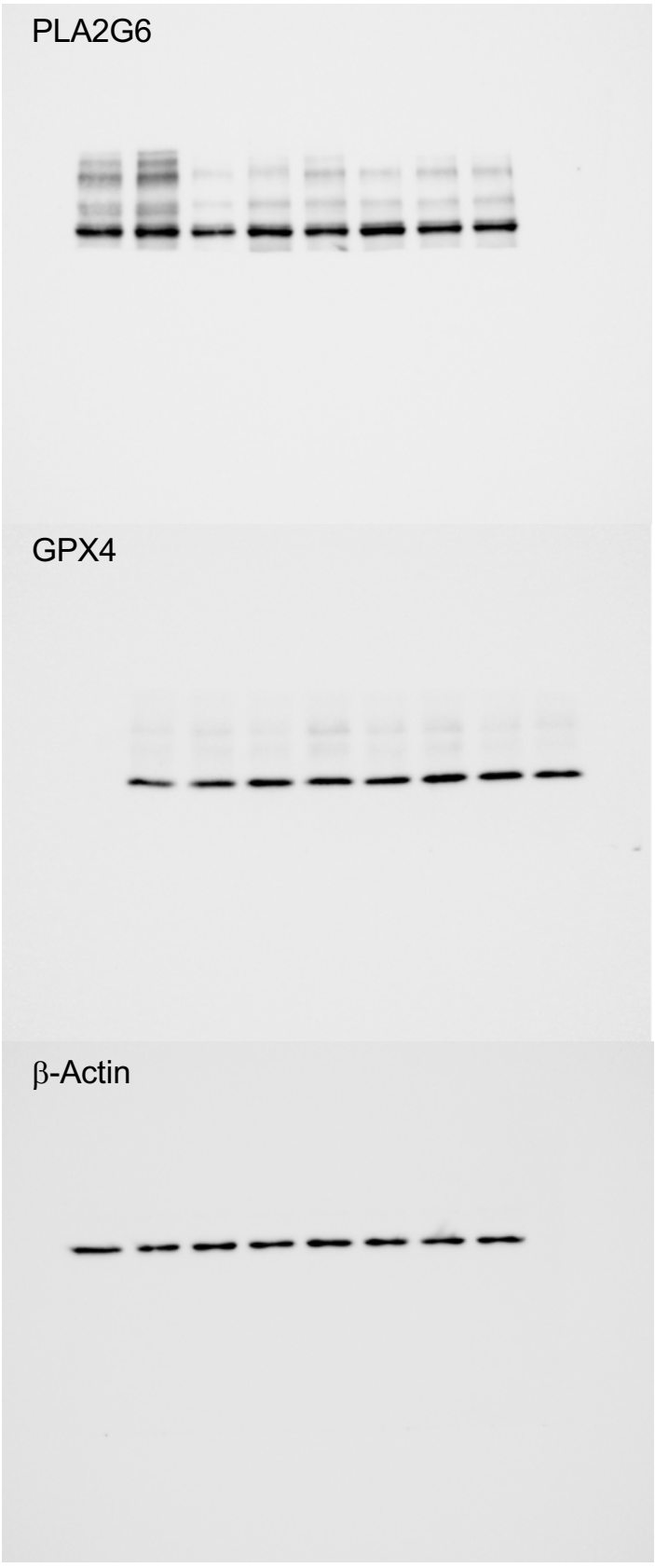

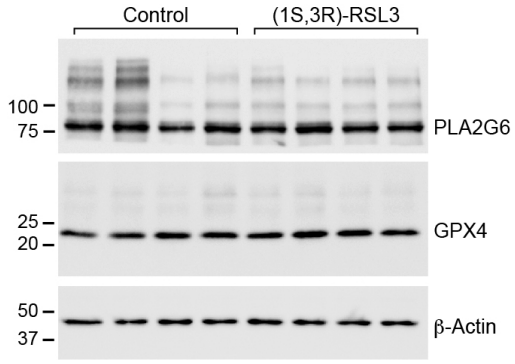

Files:
V vs RSL ANTI PLA2G6
V vs RSL ANTI GPX4 Chemiluminescence
ofer 2020-01-17 11h30m23s(Chemiluminescence)

SI Appendix, Fig. S10

PLA2G6

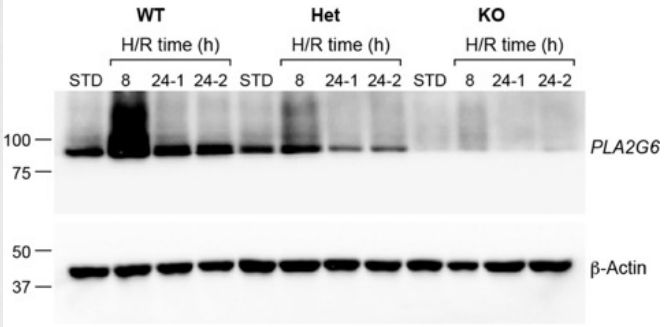

Files:
PNPLA9_2 Chemiluminescence
actin from 9 and 2-Chemiluminescence
WB Pnpla9 2actin + markers

β-Actin